Available online at www.sciencedirect.com
SCIENCE DIRECT®
Journal of Non-Crystalline Solids 343 (2004) 154–158
JOURNAL OF NON-CRYSTALLINE SOLIDS
www.elsevier.com/locate/jnoncrysol

Letter to the Editor

# Radiative transition quantum efficiency of $^2H_{11/2}$ and $^4S_{3/2}$ states of trivalent erbium ion in oxyfluoride tellurite glass

Yang Zhanci [a,*], Huang Shihua [a], Lü Shaozhe [b], Chen Baojiu [b]

[a] *Institute of Optoelectronic Technology, Beijing Jiaotong University, Beijing 100044, People's Republic of China*
[b] *Laboratory of Excited State Processes, Changchun Institute of Optics, Fine Mechanics and Physics, Chinese Academy of Sciences, Changchun 130023, China*

Received 30 December 2003; received in revised form 27 May 2004

**Abstract**

The optical transition intensity parameters of erbium ion in oxyfluoride tellurite glass were derived by fitting the absorption spectrum according to Judd–Ofelt theory. With the obtained parameters the radiative transition rates, branching ratios and lifetimes of different states in $Er^{3+}$ doped oxyfluoride tellurite glass were calculated. Temperature dependences of the emission spectrum and the lifetime of $^2H_{11/2}$, $^4S_{3/2}$ were measured within the temperature range from 108 to 315 K. The method for calculating the radiative transition quantum efficiency of the $^2H_{11/2}$ and $^4S_{3/2}$ states, which are in thermal equilibrium, was discussed. The quantum efficiencies of the $^2H_{11/2}$ and $^4S_{3/2}$ states of $Er^{3+}$ in oxyfluoride tellurite glass were calculated.


*PACS:* 71.20.Eh; 78.55.Qr

## 1. Introduction

Since up-conversion fluorescence in a tellurite matrix was observed for the first time in $Er_2O_3$ doped $70TeO_2$–$30Na_2O$ glass at room temperature [1], the up-converted green emission corresponding to $^2H_{11/2}$, $^4S_{3/2} \rightarrow {}^4I_{15/2}$ transition of the trivalent erbium ion has been extensively investigated [2,3]. The energy gap between $^2H_{11/2}$ and $^4S_{3/2}$ is about some hundreds wavenumbers, which is in the range of phonon energy. Thus, as it is well known, the $^4S_{3/2}$ and $^2H_{11/2}$ levels are always in thermal equilibrium [4]; the relative intensity of the $^4S_{3/2}$ and $^2H_{11/2}$ emissions is temperature dependent. However, little attention has been paid to the radiative transition quantum efficiency of the $^2H_{11/2}$, $^4S_{3/2}$ states.

In our work, we have investigated the temperature dependence of the radiative transition quantum efficiencies of the $^2H_{11/2}$, $^4S_{3/2}$ states. Absorption spectrum of the sample at room temperature has been measured and analyzed using the Judd–Ofelt theory. Emission spectra and decay curves of $^2H_{11/2}$, $^4S_{3/2}$ states have been measured at different temperatures ranged from 108 to 329 K. Based on these experiments, the method for evaluating the quantum efficiency of the $^2H_{11/2}$ and $^4S_{3/2}$ states has been discussed.

## 2. Experiment

The tellurite glass sample used in our measurement is with a mol% composition of $70TeO_2$–$9PbF_2$–$10AlF_3$–$10BaF_2$–$1Er_2O_3$. The raw materials of the fluoride and telluride are of analytic purity, the erbium oxide is of spectroscopic purity. Accurately weighed 10 g batches are fully mixed and moved into an alumina crucible.

* Corresponding author. Tel: +10 51683414/86105168908; fax: +10 51688018/861051688018.
*E-mail address:* shhuang@center.njtu.edu.cn (Y. Zhanci).

0022-3093/$ - see front matter © 2004 Elsevier B.V. All rights reserved.
doi:10.1016/j.jnoncrysol.2004.05.015

Then, put them into a muffle stove when the temperature of the stove rises to 800 °C and keep this temperature for 15 min. The melts are cast into a stainless steel plate and annealed at 100 °C. Samples for the optical property measurement are cut and polished to the thickness of 2 mm.

Optical absorption spectrum in the ultraviolet, visible and near infrared regions is measured by a spectrophotometer (Perkin–Elmer Lambda 9 UV/VIS /NIS/NIR) at room temperature. The refractive indices of the sample are obtained by a variable angle incidence spectroscopic ellipsometer (M-2000 J.A.Woollam Co, Inc. USA). In the measurement of the emission spectra, the sample is excited by 355 nm, the third harmonic from a QuantaRay DCR2A YAG:Nd pulsed laser. The emission is dispersed by a computer-controlled double-grating monochromator (SPEX-1403) and detected by a photomultiplier tube (Hamamatsu R945). The signal from the detector passes through a PARC 162 boxcar and is processed by a computer. The fluorescence decay curves are measured by a digital oscilloscope (Tektronix TDS3052 500 MHz). The sample is mounted in a cryostat for temperature-dependent studies.

## 3. Results

### 3.1. Judd–Ofelt parameters, radiative transition lifetime and branching ratios

Fig. 1 shows the absorption spectrum of erbium ion in $70TeO_2$–$9PbF_2$–$10AlF_3$–$10BaF_2$–$1Er_2O_3$ glass at room temperature. Ten peaks in the absorption spectrum correspond to the $^4I_{15/2} \rightarrow {}^2H_{9/2}$, $^4F_{3/2}$, $^4F_{5/2}$, $^4F_{7/2}$, $^2H_{11/2}$, $^4S_{3/2}$, $^4F_{9/2}$, $^4I_{9/2}$, $^4I_{11/2}$, $^4I_{13/2}$ absorption transitions, respectively. Fig. 2 is the dependence of the refractive index on the wavelength of the incident light. With these experimental data and Judd–Ofelt theory [5,6], we obtained the intensity parameters as $\Omega_2 = 6.74 \times 10^{-20}$, $\Omega_4 = 1.88 \times 10^{-20}$ and $\Omega_6 = 1.54 \times 10^{-20}$ cm$^2$, with rms deviation $\delta = 23 \times 10^{-22}$ cm$^2$. With the $\Omega$s, we calculate the radiative transition rates, lifetimes and branching ratios of various energy levels. The results are shown in Table 1.

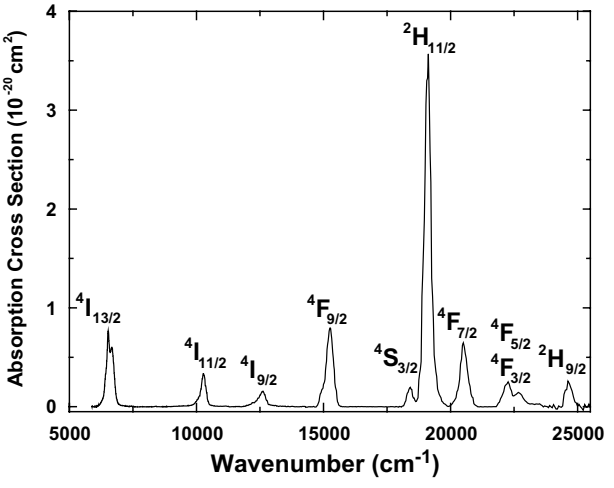


Fig. 1. Absorption spectrum of $Er^{3+}$ doped oxyfluoride tellurite glass of molar composition $70TeO_2$–$9PbF_2$–$10AlF_3$–$10BaF_2$–$1Er_2O_3$.

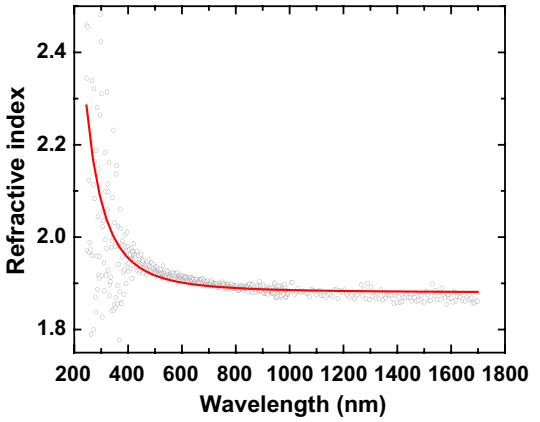


Fig. 2. The dependence of the refractive index on the wavelength of incident light.

### 3.2. Temperature dependence of green emission of the $^2H_{11/2}$, $^4S_{3/2}$ state

Fig. 3 shows the emission spectra of the $^2H_{11/2}$, $^4S_{3/2} \rightarrow {}^4I_{15/2}$ transitions at 99 K and 288 K, respectively. At 99 K, the emission from 18 600 to 19 500 wavenumbers corresponding to $^2H_{11/2} \rightarrow {}^4I_{15/2}$ is hardly observed. With the temperature increasing, the fluorescence intensity of the $^2H_{11/2} \rightarrow {}^4I_{15/2}$ transition is enhanced gradually. At 288 K, it can be observed clearly. $^2H_{11/2}$ and $^4S_{3/2}$ states, in thermal equilibrium, decay with the same rate [7–11]. Because they have different radiative transition rates, the decay rate will change with temperature. The lifetime of the fluorescence can be expressed as [7–11]

$$\tau(T) = \frac{1}{W_0 + W_1 e^{-\Delta E/kT}}, \quad (1)$$

where $W_0$ is the transition rate of the $^4S_{3/2}$ state, including radiative and non-radiative transitions, $W_1$ denotes the transition rate of the $^2H_{11/2}$ state, $\Delta E$ is the energy gap between two energy levels [7–11].

Fig. 4 shows the fluorescence decay curves monitored at 552 nm at different temperatures. Fitting the experimental curves with an exponential decay function, we obtained the luminescence decay lifetimes of the $^2H_{11/2}$, $^4S_{3/2}$

Table 1
The oscillator strengths, transition probabilities, branch ratios and lifetimes of the $Er^{3+}$ states in oxyfluoride tellurite glass

| Initial state | Final state | Wave-number | Oscillator strength ($10^{-8}$) | | Transition rate ($S^{-1}$) | | Branch ratio (%) | Lifetime (ms) |
|---|---|---|---|---|---|---|---|---|
| | | | ED | MD* | ED | MD* | | |
| $^2H_{11/2}$ | $^4S_{3/2}$ | 754 | 4.72 | | 0.06 | | 0 | 0.06 |
| | $^4F_{9/2}$ | 3882 | 160.76 | | 57.09 | | 0.34 | |
| | $^4I_{9/2}$ | 6740 | 202.58 | | 217.25 | | 1.29 | |
| | $^4I_{11/2}$ | 8991 | 80.08 | | 153.18 | | 0.91 | |
| | $^4I_{13/2}$ | 12625 | 71.88 | | 272.79 | | 1.63 | |
| | $^4I_{15/2}$ | 19120 | 1798.54 | | 16025.36 | | 95.81 | |
| $^4S_{3/2}$ | $^4F_{9/2}$ | 3128 | 5.38 | | 1.24 | | 0.03 | 0.62 |
| | $^4I_{9/2}$ | 5986 | 157 | | 132.73 | | 3.47 | |
| | $^4I_{11/2}$ | 8237 | 51.36 | | 82.39 | | 2.15 | |
| | $^4I_{13/2}$ | 11871 | 306.88 | | 1027.95 | | 26.92 | |
| | $^4I_{15/2}$ | 18366 | 314.17 | | 2573.07 | | 67.4 | |
| $^4F_{9/2}$ | $^4I_{9/2}$ | 2858 | 47.27 | | 9.09 | | 0.29 | 0.32 |
| | $^4I_{11/2}$ | 5109 | 84.56 | | 52.05 | | 1.67 | |
| | $^4I_{13/2}$ | 8743 | 82.68 | | 149.5 | | 4.79 | |
| | $^4I_{15/2}$ | 15238 | 521.94 | | 2905.93 | | 93.24 | |
| $^4I_{9/2}$ | $^4I_{11/2}$ | 2251 | 16.49 | 32.68 | 1.96 | 3.90 | 1.50 | 2.63 |
| | $^4I_{13/2}$ | 5885 | 127.71 | | 104.35 | | 27.44 | |
| | $^4I_{15/2}$ | 12380 | 74.21 | | 270.66 | | 71.06 | |
| $^4I_{11/2}$ | $^4I_{13/2}$ | 3634 | 130.91 | 58.48 | 40.73 | 18.20 | 15.65 | 2.66 |
| | $^4I_{15/2}$ | 10129 | 130.59 | | 317.52 | | 84.35 | |
| $^4I_{13/2}$ | $^4I_{15/2}$ | 6493 | 202.27 | 67.80 | 201.30 | 67.46 | 100.00 | 3.72 |

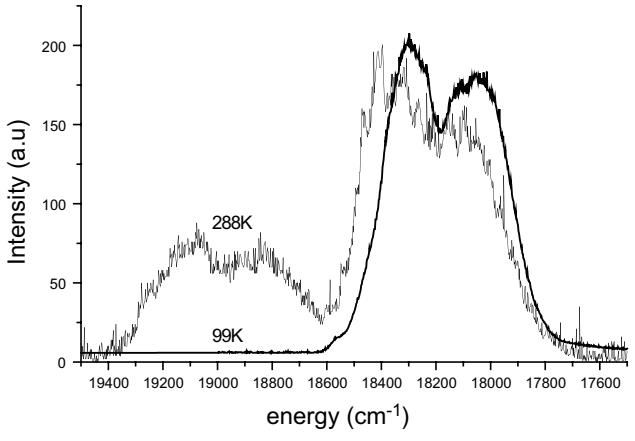


Fig. 3. The emission spectra of $^2H_{11/2}$, $^4S_{3/2} \rightarrow {}^4I_{15/2}$ at 99 K and 288 K, respectively.

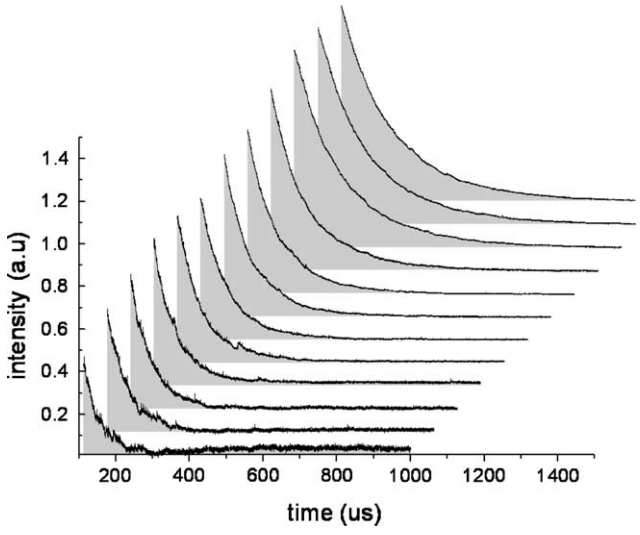


Fig. 4. The decay curves of 552 nm at different temperature, the temperatures from inside to outside is 108 K, 118 K, 127 K, 179 K, 205 K, 219 K, 235 K, 248 K, 262 K, 275 K, 287 K, 301 K, the data of the lifetimes are listed in Table 2.

states. The dependence of the lifetime on the temperature is shown in Fig. 5 together with the fitting curve according to Eq. (1). The fitting parameters are $W_0 = 666.8\,s^{-1}$, $W_1 = 2.89 \times 10^4\,s^{-1}$, $\Delta E = 611\,cm^{-1}$. From these parameters, the lifetime of the $^4S_{3/2}$ state at low temperature is $1/W_0 = 1.50$ ms, and the transition rate of the $^2H_{11/2}$ state is about 40 times larger than that of the $^4S_{3/2}$ state.

## 4. Discussions

Quantum efficiency $\eta$ is an important parameter for a luminescence material. It can be expressed as

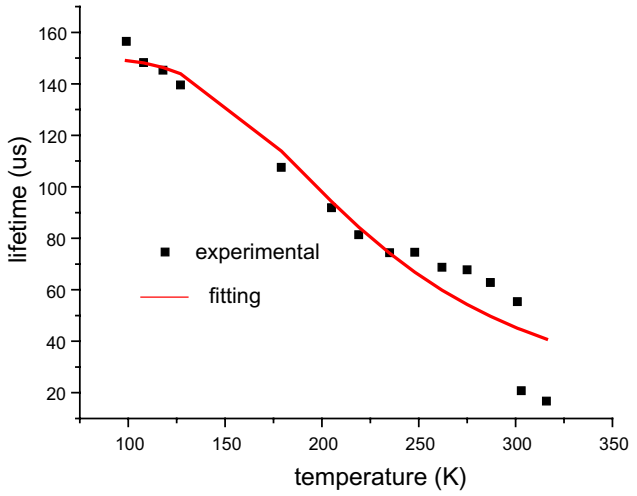


Fig. 5. Relationship between fluorescence lifetime and temperature.

$$\eta = \frac{\text{Number of photons generated in the radiative transition}}{\text{Number of electrons excited to the excited state}}. \tag{2}$$

In rare-earth luminescence materials, $\eta$ is always depicted as

$$\eta = \frac{\tau_{\text{exp}}(T)}{\tau_{\text{cal}}(T)}, \tag{3}$$

where $\tau_{\text{exp}}$ and $\tau_{\text{cal}}$ denote the experimental lifetime and the radiative transition lifetime calculated by the Judd–Ofelt theory. However, it is invalid in our case where the $^2H_{11/2}$ and $^4S_{3/2}$ states are in thermal equilibrium, since the measured decay time is not caused merely by an individual state [7–11]. Among $N$ electrons on the $^2H_{11/2}$ and $^4S_{3/2}$ states, the numbers of electrons depopulated through the $^2H_{11/2}$ state is

$$Ne^{-\Delta E/kT}\int_0^\infty W_1 \exp[-(W_0 + e^{-\Delta E/kT}W_1)t]dt = \frac{NW_1 e^{-\Delta E/kT}}{W_0 + e^{-\Delta E/kT}W_1},$$

while that through the radiative transition of the $^2H_{11/2}$ state is

$$\frac{NA_{r1}e^{-\Delta E/kT}}{W_0 + e^{-\Delta E/kT}W_1},$$

where $A_{r1}$ denotes the radiative transition rate of the $^2H_{11/2}$ state. So, the radiative transition quantum efficiency of the $^2H_{11/2}$ state can be expressed as $A_{r1}/W_1$. By analogy, the radiative transition quantum efficiency of the $^4S_{3/2}$ state can be expressed as $A_{r0}/W_0$, where $A_{r0}$ is the radiative transition rate of the $^4S_{3/2}$ state. That is, in evaluating the quantum efficiencies of $^4S_{3/2}$ and $^2H_{11/2}$, instead of the experimental $\tau_{\text{exp}}$, we should use $1/W_0$ and $1/W_1$ obtained from the fitting.

System having small energy gap like the $^2H_{11/2}$ and $^4S_{3/2}$ states also can be treated as a whole to calculate their radiative transition quantum efficiency. Among these $N$ electrons on the $^2H_{11/2}$ and $^4S_{3/2}$ states, the number of electrons depopulated via radiative transition is

$$\frac{N(A_0 + A_1 e^{-\Delta E/kT})}{W_0 + e^{-\Delta E/kT}W_1}.$$

Table 2
The calculated radiative transition rates, measured lifetimes, and the quantum efficiencies of the $^4S_{3/2}$, $^2H_{11/2}$ states at different temperatures

| Temperature (K) | $A_{r0} + A_{r1}e^{-\Delta E/kT}$ ($s^{-1}$) | $\tau_{\text{exp}}$ (μs) | Quantum efficiency (%) |
|---|---|---|---|
| 99 | 3820 | 156.49 | 56.8 |
| 108 | 3822 | 148.24 | 56.6 |
| 118 | 3827 | 145.26 | 55.6 |
| 127 | 3834 | 139.52 | 53.5 |
| 179 | 3940 | 107.48 | 42.3 |
| 205 | 4046 | 91.88 | 37.2 |
| 219 | 4118 | 81.34 | 33.5 |
| 235 | 4213 | 74.38 | 31.3 |
| 248 | 4299 | 74.55 | 32.1 |
| 262 | 4399 | 68.69 | 30.2 |
| 275 | 4499 | 67.76 | 30.5 |
| 287 | 4597 | 62.79 | 28.9 |
| 301 | 4716 | 55.34 | 26.1 |
| 303 | 4734 | 20.77 | 9.8 |
| 316 | 4850 | 16.68 | 8.1 |
| 329 | 4933 | 19.87 | 9.8 |

So the radiative transition quantum efficiency can be written as

$$\eta(T) = \frac{A_{r0} + A_{r1}e^{-\Delta E/kT}}{W_0 + W_1 e^{-\Delta E/kT}} = \tau_{exp}(A_{r0} + A_{r1}e^{-\Delta E/kT}). \quad (4)$$

With Eq. (4), the quantum efficiencies of the sample at different temperature can be obtained. The results are showed in Table 2.

## 5. Conclusions

The optical transition intensity parameters of erbium ion in oxyfluoride tellurite glass are obtained by fitting the absorption spectrum with Judd–Ofelt theory. The intensity parameters are $\Omega_2 = 6.74 \times 10^{-20}\,cm^2$, $\Omega_4 = 1.88 \times 10^{-20}\,cm^2$ and $\Omega_6 = 1.54 \times 10^{-20}\,cm^2$. With the obtained parameters, the radiative transition rates, branching ratios and lifetimes of different states in $Er^{3+}$ doped oxyfluoride tellurite glass are calculated. Emission spectra and fluorescence decay curves at different temperature are measured. With the method discussed, we calculate the radiative quantum efficiency of the $^2H_{11/2}$, $^4S_{3/2}$ states of erbium ion at different temperature.

## Acknowledgments

This work was supported by the National Science Foundation of China (Grant No. 50102006), and the State Key Project of Basic Research of China (Grant No. G1998061309).

## References

[1] S. Tanabe, K. Hirao, N. Soga, J. Non-Cryst. Solids 122 (1990) 79.
[2] D.C. Yeh, W.A. Sibley, I. Schneider, R.S. Afzal, J. Appl. Phys. 69 (1991) 1648.
[3] B.R. Reddy, P. Venkateswarlu, J. Appl. Phys. Lett. 64 (1994) 1327.
[4] V.K. Bogdanov, D.J. Booth, W.E.K. Gibbs, J. Non-Cryst. Solids 311 (2002) 48.
[5] B.R. Judd, J. Phys. Rev. 127 (1962) 750.
[6] G.S. Ofelt, J. Chem. Phys. 37 (1962) 511.
[7] S.H. Huang, Luminescence dynamics of ion centers, Science, Beijing, 2002, p. 22.
[8] S.Z. Lü, B.J. Chen, S.H. Huang, J. Acta, Phys. Sin. 52 (2003) 1009.
[9] T. Miyakawa, D.L. Dexter, J. Phys. Rev. B 1 (1970) 2961.
[10] C.W. Struck, W.H. Fonger, J. Chem. Phys. 60 (1974) 1988.
[11] M.J. Weber, J. Phys. Rev. B 8 (1973) 54.